Current Optics and Photonics
Vol. 3, No. 6, December 2019, pp. 571-576

ISSN: 2508-7266(Print) / ISSN: 2508-7274(Online)
DOI: https://doi.org/10.3807/COPP.2019.3.6.571

Identification of Fungus-infected Tomato Seeds Based on Full-Field Optical Coherence Tomography

Bharti, Taeil Yoon and Byeong Ha Lee*

School of Electrical Engineering and Computer Science, Gwangju Institute of Science and Technology (GIST), Gwangju 61005, Korea

(Received July 22, 2019 : revised September 19, 2019 : accepted September 19, 2019)

The morphological changes of anthracnose (fungus) -infected tomato seeds have been studied to identify the infection and characterize its effect. Full-field optical coherence tomography (FF-OCT) has been utilized as a nondestructive but efficient modality for visualizing the effects of fungal infection. The cross-sectional images extracted from a stack of *en face* FF-OCT images showed significant changes with infection in the seed structure. First of all, the seed coat disappeared with the infection. The thickness of the seed coat of a healthy seed was measured as 28.2 μm, with a standard deviation of 1.2 μm. However, for infected seeds the gap between surface and endosperm was not appreciably observed. In addition, the measurements confirmed that the dryness of seeds did not affect the internal seed structure. The reconstructed three-dimensional (3D) image revealed that the permeability of the seed coat, which plays the vital role of protecting the seed, is also affected by the infection. These results suggest that FF-OCT has good potential for the identification of fungus-infected tomato seeds, and for many other tasks in agriculture.

Keywords : Anthracnose, Seed structure, Optical imaging, Full-Field OCT
OCIS codes : (170.3880) Medical and biological imaging; (170.4500) Optical coherence tomography

I. INTRODUCTION

A seed is a small embryonic plant enclosed in a covering, called the *seed coat*, usually with some stored food, or *endosperm*, providing nutrition for the embryo's development. The seed coat is a protective barrier, ensuring protection from water, heat, disease, and parasites [1, 2]. Most agricultural practices begin and end with seeds, and the quality of seeds is crucial for healthy seedlings, good plants, and ultimately a good crop harvest. In agriculture, research on imaging the microstructure of seeds has been ongoing since 2000 [3]. Anthracnose is a fungal infection caused by the *Colletotrichum coccodes* pathogen in tomato, which spreads deeply with time and spoils the quality of fruits and their seeds [4]. As is well known, infected seeds are responsible for poor seed germination and reduce the production of fruits; they are also responsible for long-distance transport of pathogens, due to seed trading between countries [5]. These pathogens infect a number of other crops as well. In addition, they can produce some toxins due to micro-organisms such as bacteria and fungi, and cause health issues [6, 7]. With these problems, prior selection of healthy seeds becomes important in many senses. Therefore, it is necessary developing some efficient methods that can characterize infected seeds or distinguish them from the healthy ones.

Several imaging techniques have been tried in agriculture studies of plant tissues and seeds, including near-infrared reflection spectroscopy [7], light and electron microscopy [8, 9], confocal microscopy [10], x-ray tomography [11], and magnetic resonance microscopy [12]. The more conventional methods used for the detection of seedborne pathogens are well summarized in [13]; these include visual inspection of dry seeds, microscopic examination, washing test, seed soaking, seed incubation, staining test, embryo count, and many more. Each modality has merits and demerits,

*Corresponding author: leebh@gist.ac.kr, ORCID 0000-0003-4544-1232
Color versions of one or more of the figures in this paper are available online.

depending on application and practice in general. Some have high resolution, but limitations in the imaging depth. Others have good penetration, but rather poor resolution.

For seed imaging, we prefer a noncontact, nondestructive, and noninvasive modality that allows real-time tomographic imaging with high resolution. These preferences can be satisfied by optical coherence tomography (OCT) [14]. OCT has attracted the attention of many researchers, mainly in the biomedical field [15], and is extending its applications even to agriculture [16-18]. Time-domain OCT has already been used to measure hull thickness of lupine seed [3].

In this study, we inspect and characterize the structure of seeds affected by fungal infection, using full-field OCT (FF-OCT). FF-OCT is an efficient, noninvasive imaging modality based on a Michelson interferometer, but equipped with a 2D detector array such as a CCD [19]. FF-OCT provides some advantages over conventional point-scan OCT. First, because it can use an ultrabroadband light source such as a halogen lamp, we can expect even submicrometer axial resolution. Second, thanks to the use of Michelson interferometry, we can enjoy high lateral resolution by using a high-NA microscope objective, as in conventional light microscopy. In addition, by using a 2D detector array, an *en face* tomogram can be obtained without any transverse scanning. Thus, we want to clarify experimentally that the FF-OCT is an efficient and powerful modality for studying infected seeds.

II. METHOD AND EXPERIMENT

The schematic of our homemade FF-OCT system is shown in Fig. 1. As a broadband light source, a 100-W halogen lamp (KI-100W, Korea Intech) is used. It has a central wavelength of 650 nm and a spectral bandwidth of 220 nm. The light beam from the source is divided by a beam splitter (BS) into the reference and sample arms of the interferometer. In the sample arm, a sample is illuminated through a microscope objective (MO) (UMPLFL series, Olympus, Japan) having a NA of 0.3. The light backscattered from the sample is collected by the same MO, and then transferred to a CCD (CCD1020, 20 fps, 512 × 512 pixels, VDS) through the BS. In the reference arm, the beam is reflected by a reference mirror (RM) and returned to the BS through another identical MO. The RM is attached to a piezoelectric actuator (PZT) to make it oscillate at a certain frequency, 5 Hz in our case. The axial and transverse resolutions of our FF-OCT system are 1.0 and 2.2 μm respectively. The detection sensitivity of the system is 58 dB, without averaging [19].

By matching the path lengths of both arms, the CCD can capture the interference fringes. Then a series of 12-bit digitized readout signals are taken by a frame grabber (NI PCI-1428, NI). As was explained in [19], by taking 4 interference fringe images at a certain depth along the sample, but with different phases of the reference arm, one *en face* image is reconstructed. The data-acquisition process is automatically controlled using homemade LabVIEW software.

The samples used for the experiments were seeds of cherry tomatoes, prepared in our laboratory. The tomatoes were put in a plastic box; after being sealed tightly, the box was placed at room temperature until we were able to see fungal growth on the tomatoes' surfaces. Sample preparation took about two weeks, at which point we could see the visible symptom of infection: black spots on the surfaces.

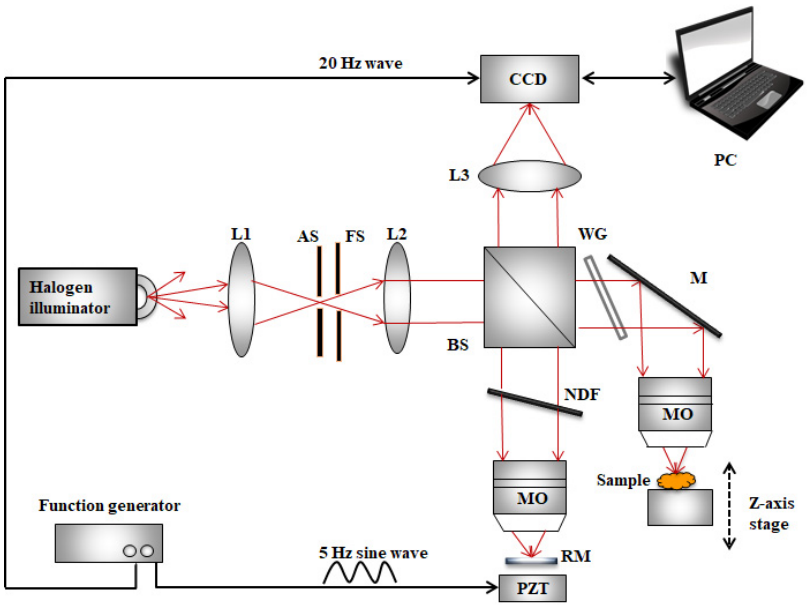

FIG. 1. Schematic of a Full-Field OCT (FF-OCT) system: L, lens; AS, aperture stop; FS, field stop; BS, beam splitter; MO, microscope objective; RM, reference mirror; WG, window glass; M, mirror; NDF, neutral density filter; PZT, piezoelectric actuator.

Contrarily, healthy seeds were brownish and shiny. 10 seeds from each of the healthy and infected lots were used for imaging. Each seed was scanned by the FF-OCT system and its cross-sectional image used for analysis of the layered structure of the seed. A FF-OCT 3D image of the sample was used to examine the impact of infection on the seed coat's surface as well. Dried and non-dried healthy seeds were also compared, to ensure whether the structural changes were due to dryness or infection. Each seed was about 3 mm long and had a thickness of 150~200 μm.

III. RESULTS AND DISCUSSION

Two sets of seed samples, one of healthy seeds and the other infected, were prepared separately, as mentioned in the previous section. Photographs of the cherry tomatoes and their seeds used for the experiment are shown in Fig. 2.

3.1. Comparison of Healthy and Infected Seeds Using FF-OCT

With the FF-OCT system of Fig. 1, *en face* tomographic images of each sample were extracted at different imaging depths, as in Figs. 3 and 4. In these figures we can see some contourlike images, which result from curved plane boundaries in the sample. As the depth increases, we can see that the contour becomes larger and larger. At a glance, we can clearly identify that the *en face* image of an infected seed is different from that of a healthy one.

To make the identification clearer, cross-sectional images were reconstructed from a stack of *en face* images and presented in Fig. 5. Interestingly, the healthy seed (Fig. 5(a)) shows two layers (boundaries), while the infected seed (Fig. 5(b)) shows just one. To confirm the layer disappearance with infection, line profiles were taken along the yellow arrows. For the healthy seed, Fig. 5(c) shows two well-separated peaks; one is for the air-seed coat layer, and the other for the seed-coat-endosperm layer. However, as in Fig. 5(d), the infected seed shows only one strong peak. Even though a second peak might exist, its signal intensity must be very weak.

The distances between two layers were measured for the 10 healthy seeds and summarized in Table 1. The average was 28.2 μm, with a standard deviation of 1.2 μm. In addition, the 3D images of the seeds reveal that the permeability (the ability for material exchange with environment [2]) of the seed coat was also affected by the infection. Figure 6 shows that the infection made some discontinuities and cavities in the seed coat, and that the surface became rather rough with the infection. Therefore, it is possible that certain undesirable materials (fungi, pathogens, moisture, or air) could penetrate the seed coat and diffuse to the seed embryo, rendering the whole seed easily infected.

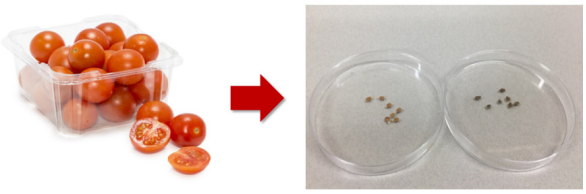

FIG. 2. Photographs of the cherry tomatoes and some of their healthy (left) and fungus-infected (right) seeds used for the experiment.

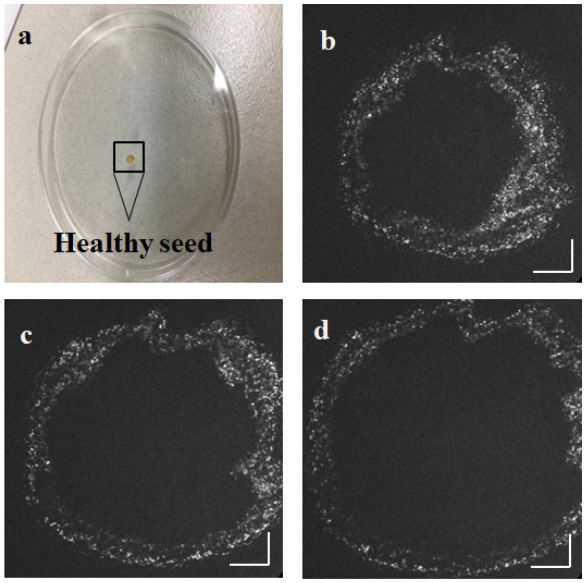

FIG. 3. *En face* images of a healthy seed (a), taken (b) 75 μm, (c) 100 μm, and (d) 125 μm below the top surface. Scale bars: horizontal, 200 μm; vertical, 50 μm.

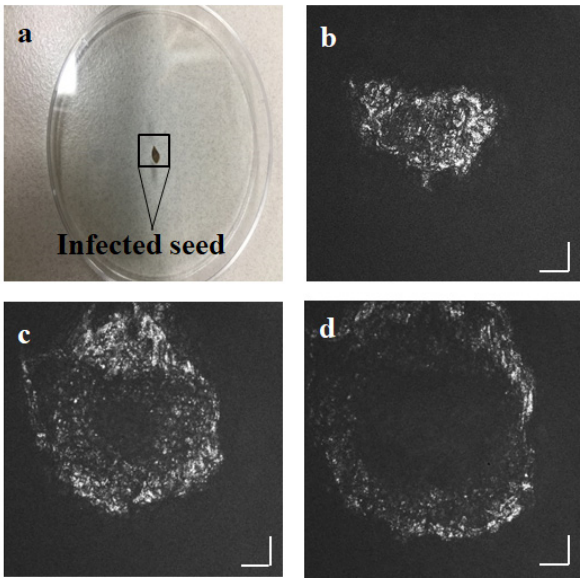

FIG. 4. *En face* images of an infected seed (a), taken (b) 75 μm, (c) 100 μm, and (d) 125 μm below the top surface. Scale bars: horizontal, 200 μm; vertical, 50 μm.

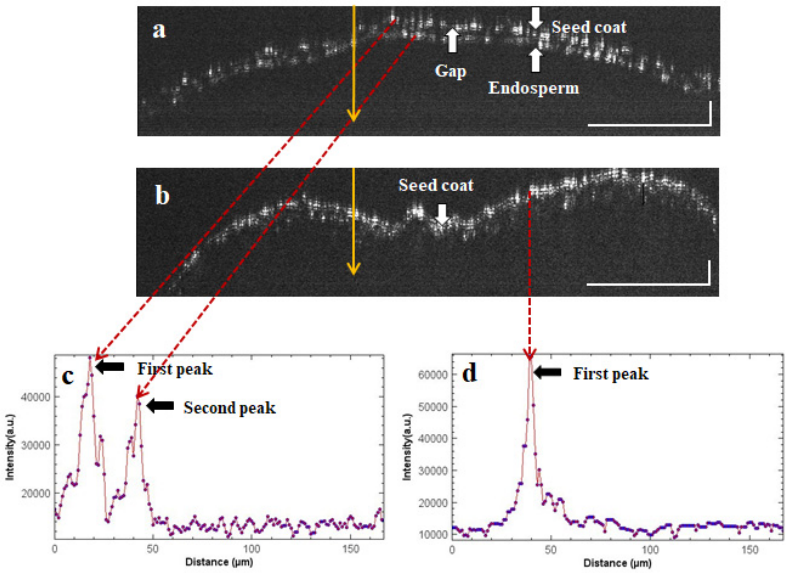

FIG. 5. FF-OCT cross-sectional images of a healthy (a) and an infected tomato seed (b), and the line profiles for the healthy seed (c) and the infected one (d). White scale bars: horizontal, 200 μm; vertical, 50 μm.

TABLE 1. Measured distances between the seed coat and the endosperm layer

Healthy seed sample No.	Average distance (μm)
1	27.3
2	28.1
3	27.5
4	29.2
5	26.2
6	29.8
7	29.4
8	26.7
9	28.2
10	30.1
Total average distance (μm)	28.17 μm
Standard deviation	1.2 μm

3.2. Comparison of Dryness between Dried and Non-dried Healthy Seed Using FF-OCT

The effect of dryness on seed imaging was also investigated. We wanted to distinguish the effect of dryness from that of infection. At first, a healthy seed was air-dried for a week at room temperature and then imaged every day for 5 days, to see the changes in the seed structure. Figure 7(b) shows the results, where we can see that the two strong layers were still present, even after drying. This means dryness did not affect the seed's structure appreciably, but infection did. From this we can conclude that dryness and time do not affect the layered structure of the tomato seed severely, but fungal infection does.

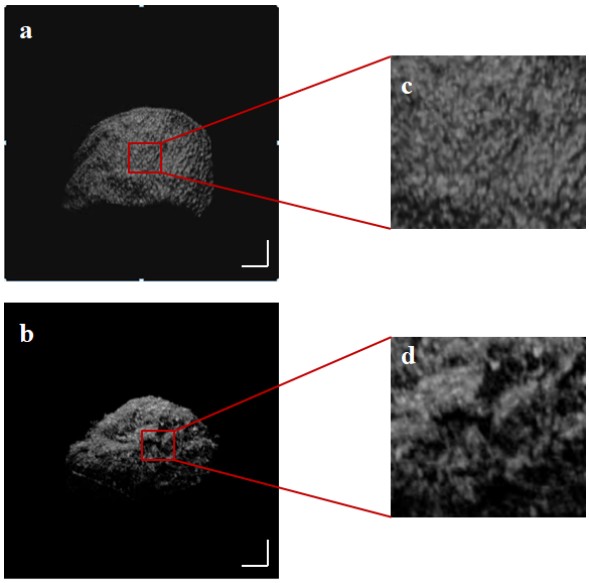

FIG. 6. FF-OCT images of the seed coat's surface for (a) healthy and (b) infected tomato seeds. (c) and (d) are their enlarged views. White horizontal and vertical scale bars are 200 μm.

However, due to the insufficient resolution of the system and the uncertainty in the imaging position of the seed sample in each measurement, a systematic comparison of the seed during the drying process could not be made clearly. It is expected that more thorough alignment and adjustment of the system's hardware would allow clearer and more distinguishable images for comparison. Furthermore, even though the five images of Fig. 7(b) were taken for the same seed, at each measurement, it was not clarified that the seed sample was placed in the same

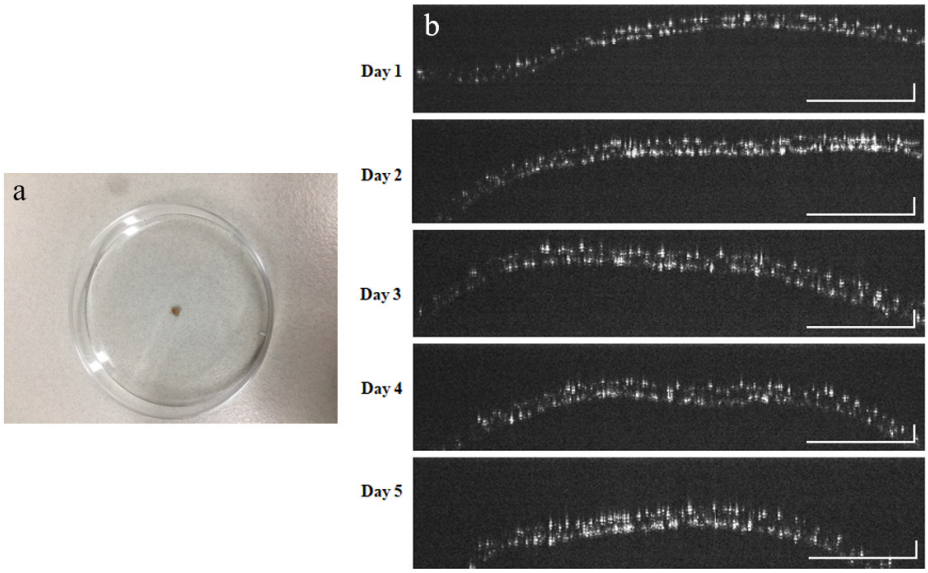

FIG. 7. FF-OCT cross-sectional images of a dried healthy seed. Using the dried healthy seed (a), images were taken for 5 days (b) after one week of drying. For each measurement, the seed sample was loaded for imaging and then removed for keeping. White scale bars: horizontal, 200 μm; vertical, 50 μm.

position and with the same orientation. We intend to devise a zig that can allow identical measurements. With the improved FF-OCT system and the dedicated zig, we want to further clarify the identification of the infected seed.

IV. CONCLUSION

We have investigated the suitability of full-field optical coherence tomography (FF-OCT) for identifying fungus-infected tomato seeds. In a healthy seed we could see two strong layers, corresponding to the seed coat and the endosperm boundaries, whereas only one layer was seen in an infected seed. The gap between the two strong layers of the healthy seed was 28.2 μm on average, with a standard deviation of 1.2 μm. The 3D structural image reconstructed from a stack of FF-OCT images revealed that the permeability of the seed coat was also affected by the infection. We could see some discontinuities and roughness in the infected seed's coat, which is thought to make the seed more permeable and susceptible to infection. We also confirmed that the dryness of the seed did not appreciably change the structure of the seed.

The FF-OCT system used for the experiment was homemade and LabVIEW controlled. The infection of the tomato seeds was also conducted in the laboratory. Some cherry tomatoes were put in a plastic box and placed at room temperature for two weeks. For the dryness experiment, some fresh seeds were placed at room temperature for a week, and after that the FF-OCT measurements were made for the next 5 days. Putting all results together, we can conclude that FF-OCT is as an efficient imaging modality to identify fungus-infected tomato seeds. In addition, it can be applicable to analysis and characterization of other agricultural crops. However, we can think of increasing the accuracy of infection diagnosis with the help of other modalities; near-infrared reflection spectroscopy and hyper-spectral spectroscopy could be good candidates.

ACKNOWLEDGMENT

This paper is supported by the GRI (GIST Researcher) project and funded by the Gwangju Institute of Science and Technology in 2019, and the National Research Foundation of Korea (NRF) grant funded by the Korean government (MSIT) (No. NRF-2019R1F1A1061859).

REFERENCES

1. F. H. D. D. Souza and J. M. Filho, "The seed coat as a modulator of seed-environment relationships in Fabaceae," Braz. J. Bot. **24**, 365-375 (2001).
2. V. Radchuk and L. Borisjuk, "Physical, metabolic and developmental functions of the seed coat," Front. Plant Sci. **5**, 510 (2014).
3. J. C. Clements, A. V. Zvyagin, K. K. M. B. D. Silva, T. Wanner, D. D. Sampson, and W. A. Cowling, "Optical coherence tomography as a novel tool for non-destructive measurement of the hull thickness of lupin seeds," Plant Breed. **123**, 266-270 (2004).
4. A. H. Wani, "An overview of the fungal rot of tomato," Mycopath **9**, 33-38 (2011).
5. F. Constable, G. Chambers, L. Penrose, A. Daly, J. Mackie, K. Davis, B. Rodoni, and M. Gibbs, "Viroid-infected tomato and capsicum seed shipments to australia," Viruses **11**, 98

(2019).
6. M. E. E. Alahi and S. C. Mukhopadhyay, "Detection methodologies for pathogen and toxins: a review," Sensors **17**, 1885 (2017).
7. J. Lim, G. Kim, C. Mo, K. Oh, H. Yoo, H. Ham, and M. S. Kim, "Classification of *Fusarium*-infected Korean hulled barley using near-infrared reflectance spectroscopy and partial least squares discriminant analysis," Sensors **17**, 2258 (2017).
8. C. H. Lin, R. H. Falk, and C. R. Stocking, "Rapid chemical dehydration of plant material for light and electron microscopy with 2,2-dimethoxypropane and 2,2-diethoxypropane," Am. J. Bot. **64**, 602-605 (1977).
9. J. M. Canne, "A light and scanning electron microscope study of seed morphology in *Agalinis* (Scrophulariaceae) and its taxonomic significance," Syst. Bot. **4**, 281-296 (1979).
10. E. Truernit and J. Haseloff, "A simple way to identify non-viable cells within living plant tissue using confocal microscopy," Plant Methods **4**, 15 (2008).
11. S. Dhondt, H. Vanhaeren, D. V. Loo, V. Cnudde, and D. Inzé, "Plant structure visualization by high-resolution X-ray computed tomography," Trends Plant Sci. **15**, 419-422 (2010).
12. J. S. Veres, G. P. Cofer, and G. A. Johnson, "Distinguishing plant tissues with magnetic resonance microscopy," Am. J. Bot. **78**, 1704-1711 (1991).
13. P. Upadhyay and S. P. Singh, "Detection methods for seed borne pathogens," Int. J. Curr. Microbiol. Appl. Sci. **8**, 318-323 (2019).
14. J. G. Fujimoto, C. Pitris, S. A. Boppart, and M. E. Brezinski, "Optical coherence tomography: an emerging technology for biomedical imaging and optical biopsy," Neoplasia **2**, 9-25 (2000).
15. J. P. Kolb, W. Draxinger, J. Klee, T. Pfeiffer, M. Eibl, T. Klein, W. Wieser, and R. Huber, "Live video rate volumetric OCT imaging of the retina with multi-MHz A-scan rates," PLoS One **14**, e0213144 (2019).
16. V. V. Sapozhnikova, V. A. Kamenskii, and R. V. Kuranov, "Visualization of plant tissues by optical coherence tomography," Russ. J. Plant Physiol. **50**, 282-286 (2003).
17. I. S. Kutis, V. V. Sapozhnikova, R. V. Kuranov, and V. A. Kamenskii, "Study of the morphological and functional state of higher plant tissues by optical coherence microscopy and optical coherence tomography," Russ. J. Plant Physiol. **52**, 559-564 (2005).
18. M. Boccara, W. Schwartz, E. Guiot, and G. Vidal, "Early chloroplastic alterations analyzed by optical coherence tomography during a harpin-induced hypersensitive response," Plant J. **50**, 338-346 (2007).
19. W. J. Choi, J. H. Na, S. Y. Ryu, B. H. Lee, and D. S. Ko, "Realization of 3-D topographic and tomographic images with ultrahigh-resolution full-field optical coherence tomography," J. Opt. Soc. Korea **11**, 18-25 (2007).